Estimating 'outbreak'-level tornado counts and casualties from environmental variables

Zoe Schroder*

Department of Geography, Florida State University, Tallahassee, FL, USA, 32306

James B. Elsner

Florida State University, Tallahassee, FL, USA, 32306

**Corresponding author*: Zoe Schroder, zms17b@my.fsu.edu

* This paper is currently under review in the journal *Weather, Climate, and Society*.

ABSTRACT

Environmental variables are routinely used in estimating when and where tornadoes are likely to occur, but more work is needed to understand how severe weather outbreak characteristics (e.g. tornado and casualty counts) vary with the larger scale environmental factors. Here the authors demonstrate a method to quantify 'outbreak'-level tornado and casualty counts with respect to variations in large-scale environmental factors. They do this by fitting negative binomial regression models to cluster-level environmental data to estimate the number of tornadoes and the number of casualties on days with at least ten tornadoes. Results show that a 1000 J kg^{-1} increase in CAPE corresponds to a 5% increase in the number of tornadoes and a 28% increase in the number of casualties, conditional on at least ten tornadoes, and holding the other variables constant. Further, results show that a 10 m s^{-1} increase in deep-layer bulk shear corresponds to a 13% increase in tornadoes and a 98% increase in casualties, conditional on at least ten tornadoes, and holding the other variables constant. The casualty-count model quantifies the decline in the number of casualties per year and indicates that outbreaks have a larger impact in the Southeast than elsewhere after controlling for population and geographic area.

1. Introduction

Estimating characteristics of severe weather outbreaks (i.e., tornado and casualty counts) is an important and challenging problem. It is important because of the potential for loss of life and property damage. It is challenging because of the uncertainties associated with exactly how many and where the tornadoes will occur. But progress is being made. Guidance from dynamical models help forecasters outline areas of possible severe weather threats days in advance (Hitchens and Brooks 2014) while guidance from statistical models help forecasters quantify probabilities for given severe weather events (Thompson et al. 2017; Cohen et al. 2018; Elsner and Schroder 2019; Hill et al. 2020). For example, Cohen et al. (2018) use a regression model to specify the probability of tornado occurrence given certain environmental and storm-scale conditions (circulation above radar level, rotational velocity, circulation diameter, etc). Elsner and Schroder (2019) extend this model by making use of the cumulative logistic link function that estimates probabilities for each damage rating using storm-relative helicity, bulk shear, and convective available potential energy (CAPE). These studies put statistical guidance for estimating severe weather outbreak characteristics on a firm mathematical foundation (Cohen et al. 2018; Elsner and Schroder 2019). Room for additional work in this area motivates the present study. For instance, the cumulative logistic regression (Elsner and Schroder 2019) provides a distribution for the *percentage* of tornadoes within each Enhanced Fujita (EF) rating category (Fujita 1981), but a model is needed to estimate the overall number of tornadoes given the likelihood of at least some tornadoes.

Tornado outbreaks pose a risk of significant loss of life and property. Anderson-Frey and Brooks (2019) consider the role environmental factors play in the number of outbreak fatalities. They use self-organizing maps on the significant tornado parameter (STP) and find that more damaging tornadoes (>EF3) present a higher risk for fatalities. However, they also note that both deadly and non-deadly tornadoes are associated with high values of STP. Self-organizing maps are useful for describing the role of environmental variables on casualties, but a statistical model is needed to quantify the relationship between casualty counts and environmental factors. Here we demonstrate a method to model 'outbreak'-level tornado and casualty counts from environmental conditions and predefined tornado clusters. The model allows us to quantify the associative relationships between environmental variables and tornado counts. Moreover, the approach might eventually help extend the available statistical guidance for predicting outbreak characteristics particularly when combined with other models.

In this paper, we focus on tornado outbreaks rather than on individual tornadoes. The larger space and time scales associated with the outbreak better matches our interest in the larger-scale environmental factors like CAPE and shear. In what follows, we call the outbreaks 'clusters' as is done in Schroder and Elsner (2019) because we make no attempt to associate the cluster with a particular synoptic-scale system. A cluster is defined (informally) as a group of ten or more tornadoes occurring over a relatively short time scale (e.g., one day) and over a relatively limited spatial domain (e.g., one to three states) (Fig. 1). Clusters in the United States are most frequent during April, May, and June (Dixon et al. 2014; Tippett et al. 2012; Dean 2010) with most of them occurring across the Central Plains and the Southeast. Clusters are less common in the Southeast and the Southern Plains during the summer months as the jet stream migrates north taking the necessary wind shear with it (Concannon et al. 2000; Gensini and Ashley 2011; Jackson and Brown 2009). The percentage of all tornadoes occurring in clusters has recently been found to be increasing over time (Moore 2017; Tippett et al. 2016; Elsner et al. 2015; Brooks et al. 2014).

This paper has two objectives: (1) demonstrate that environmental conditions prior to the occurrence of any tornadoes can be used to skillfully model the number of tornadoes in a cluster containing at least ten tornadoes (tornado-count model), and (2) show that these same environmental conditions can be used to estimate the number of casualties if the number of people in harm's way is known (casualty-count model). We accomplish these objects by fitting negative binomial regressions to cluster-level tornado data. The cluster-level data are environmental variables and tornado characteristics (e.g., number of tornadoes, number of casualties, etc) on convective days (12 UTC to 12 UTC), when the number of tornadoes is at least ten [see Elsner and Schroder (2019)]. The paper is outlined as follows. The data and methods are discussed in section 2 including the mathematics of a negative binomial regression. Statistics describing the response (i.e., tornado-casualty counts) and environmental variables are given in section 3. The modeling results are presented in section 4, and a summary with conclusions are given in section 5.

2. Data and methods

We fit regression models to a set of tornado and reanalysis data aggregated to the level of tornado clusters. Here we describe how we organize the data and the procedures to aggregate values to the cluster level. For our purposes, a cluster is a group of at least ten tornadoes occurring relatively close to one another in both space and time between 12 UTC and 12 UTC. Ten is chosen as a compromise between too few clusters leading to greater uncertainty and too many clusters leading to excessive time required to fit the models (Elsner and Schroder 2019). Ten is also the number that is sometimes used formally to define an outbreak (Galway 1977; Anderson-Frey et al. 2018). The number of tornadoes in each cluster is the response variable in the tornado-count regression model, and the number of casualties is the response variable in the casualty-count regression model. Explanatory variables include outbreak size and location as well as environmental variables from reanalysis data representing conditions before the occurrence of the first tornado in the cluster.

a. Tornado clusters

First, we extract the date, time, genesis location, and magnitude of all tornado reports between 1994 and 2018 from the Storm Prediction Center [SPC] (`https://www.spc.noaa.gov/gis/svrgis/`). We choose 1994 as the start year because it is the first year of the extensive use of the WSR-88D Radar (Heiss et al. 1990). In total, there are 30,497 national tornado reports during this period. The geographic coordinates for each genesis location are converted to Lambert conic conformal coordinates, where the projection is centered on 96° W longitude.

Next, we assign to each tornado a cluster identification number based on the space and time differences between genesis locations. Two tornadoes are assigned the same cluster identification number if they occur close together in space and time (e.g., 1 km and 1 h). When the difference between individual tornadoes and existing clusters surpasses 50,000 s (∼ 14 h), the clustering ends. The space-time differences have units of seconds because we divide the spatial distance by 15 m s^{-1} to account for the average speed of tornado-producing storms. This speed is commensurate with the magnitude of the steering-level wind field across the clusters. The clustering is identical to that used in Elsner and Schroder (2019) who developed a cumulative logistic model to the damage scale at the individual tornado level. Additional details on the procedure, as well as a comparison of the identified clusters to well-known outbreaks, are available in Schroder and Elsner (2019).

We keep only clusters having at least ten tornadoes occurring within the same convective day (12 - 12 UTC), which results in 768 clusters with a total of 17,069 tornadoes. The average number of tornadoes per cluster is 22 and the maximum is 173 (April 27, 2011). There are 80 clusters with exactly ten tornadoes. Each cluster varies by area and by where it occurs geographically (see Fig. 1 for examples of clusters). The cluster area is defined by the minimum convex hull (black polygon) that includes all the tornado genesis locations. The July 19, 1994 cluster with nine tornadoes over northern Iowa and one over northwest Wisconsin had an area of 33,359 km^2 and lasted about four hours. The April 27, 2011 cluster had 173 tornadoes spread over more than a dozen states and had an area of 1,064,337 km^2 with tornadoes occurring throughout the 24-h period (12-UTC to 12-UTC).

For each cluster we sum the number of injuries and deaths across all tornadoes to get the cluster-level number of casualties (sum of injuries and fatalities). Further we estimate the population within the cluster area and the geographic center of the cluster. Population values are U.S. Census Bureau estimates in cities with at least 40,000 people (Steiner 2019). Population is used as an explanatory variable in place of cluster area in the casualty-count model.

b. Environmental variables

Large-scale environmental conditions for producing tornadoes are well studied and include large magnitudes of convective available potential energy, bulk shear, and weak convective inhibition (Brooks et al. 1994; Rasmussen and Blanchard 1998; Thompson et al. 2003; Shafer and Doswell 2011; Doswell et al. 2006). We obtain variables associated with these environmental conditions from the National Centers for Atmospheric Research's North American Regional Reanalysis (NARR), which is supported by the National Centers for Environmental Prediction (Mesinger et al. 2006). Each variable has numeric values given on a 32-km raster grid with the values available in three-hour increments starting at 00 UTC. In the severe weather literature, these environmental variables are called 'parameters'. However here, since we employ statistical models, we call them variables to be consistent with the statistical literature where the word 'parameter' denotes unknown model coefficients and moments of statistical distributions (e.g., the mean).

We select environmental variables at the nearest three-hour NARR time *prior* to the occurrence of the first tornado in the cluster. For example, if the first tornado in a cluster occurs at 16:30

UTC we use the environmental variables given at 15 UTC. This selection criteria results in a sample of the environment that is less contaminated by the deep convection itself but at a cost that underestimates the severity in cases where environmental conditions rapidly change favoring tornado development. About 60% of all clusters have the initial tornado occurring between 18 and 00 UTC (Table 1). However, there are more tornadoes in clusters when the first tornado occurs between 15 and 18 UTC on average.

The environmental variables we consider include convective available potential energy (CAPE) and convective inhibition (CIN) as computed using the near-surface layer (0 to 180 mb above the ground level) consistent with Allen et al. (2015b). We also include deep (1000 to 500 mb) and shallow (1000 to 850 mb) layer bulk shears (DLBS, SLBS) computed as the square root of the sum of the squared differences between the u and v wind components at the respective levels consistent with Tippett et al. (2012). Climate researchers use these NARR variables at the climatological scale as proxies for the more traditional variables used in forecasting severe weather (Allen et al. 2015b; Moore et al. 2016; Tippett et al. 2012). We take the highest (lowest for CIN) value across the grid of values within the area defined by the cluster's convex hull. This is done to capture environmental conditions that represent the unadulterated pre-tornado environment. In contrast, the mean (or median) value is influenced by conditions throughout the domain including earlier occurring non-tornado-producing convection and in areas within the clusters that did not experience tornado activity. Histograms of the maximums (not shown) show no evidence of extreme behavior.

Storm-relative helicity is not used because it is correlated with DLBS and SLBS (Table 2). Likewise dew-point temperature and specific humidity are not used because of their relatively high correlation with CAPE. Further we do not use composite variables including the significant tornado parameter (STP) and the supercell composite parameter (SCP). STP, for example, is the product of variables including CAPE, storm-relative helicity, CIN, and lifted condensation level

(LCL) height. A moderate value of STP can result from either high CAPE and low shear or low CAPE and high shear environments holding the other variables constant. Here we separate this composite relationship to examine the direct relationships between CAPE and shear on tornado activity at the scale of outbreaks.

c. Negative binomial regression

With the cluster as our unit of analysis, we fit a series of regression models to the data having the form

$$
\begin{aligned}
T &\sim \mathrm{NegBin}(\hat{\mu}, n) \\
\ln(\hat{\mu}) &= \beta_0 + \beta_A A + \beta_\phi \phi + \beta_\lambda \lambda + \beta_Y Y + \\
&\quad \beta_{CAPE}\mathrm{CAPE} + \beta_{CIN}\mathrm{CIN} + \beta_{DLBS}\mathrm{DLBS} + \beta_{SLBS}\mathrm{SLBS},
\end{aligned} \tag{1}
$$

where the number of tornadoes (T) is the dependent variable that is assumed to be adequately described by a negative binomial distribution (NegBin) with a rate parameter μ and a size parameter n (Hilbe 2011). The natural logarithm of the rate parameter is linearly related to cluster area (A), cluster center location [latitude (ϕ) and longitude (λ)], year (Y) and the four environmental variables (CAPE, CIN, DLBS, and SLBS). These are the explanatory variables. The model is fit using the method of maximum likelihoods carried out in the call to the `glm.nb` function from `MASS` package in R (Venables and Ripley 2002). We do the same for the initial casualty-count model, but we replace cluster area with population (P). We simplify the initial models through single-term deletions as described in §4.

Regression model skill is evaluated using the observed counts and the predicted rates. The predicted rates for each cluster are obtained by plugging the values of the associated explanatory variables into the model. Predicted rates are under dispersed (lower variation) relative to the observed counts. Comparisons are made using the metrics of Pearson correlation coefficient and mean absolute error. Predictive skill using these metrics is evaluated using in-sample and out-of-sample predictions. In-sample predictions are made using all clusters to fit a single model while out-of-sample predictions are made by successively holding one cluster out of the model fitting procedure and using the particular model to predict the counts from the cluster left out [hold-one-out cross validation; see Elsner and Schmertmann (1994)].

3. Results

a. Descriptive statistics

The number of clusters decreases exponentially with an increasing number of tornadoes per cluster (Fig. 2). There are 80 clusters with ten tornadoes but only ten clusters with 30 tornadoes. The right tail of the count distribution is long with the April 27, 2011 cluster having 173 tornadoes [47 (6%) of the clusters have more than 50 tornadoes and are not shown]. However more clusters have 20 or 21 tornadoes than expected from a simple decay function. This deviation is unlikely the result of physical processes, and it appears too large to be sampling variability. It might be due to a consistent rounding of the totals to the nearest five or ten. There is an upward trend in the number of tornadoes per cluster (not shown) consistent with recent studies (Elsner et al. 2015). The distribution of casualties is also skewed toward many clusters having only a few casualties and a few have many. Thirty-six percent of all clusters (275) are without a casualty and 56% of the clusters have fewer than four casualties.

There is a seasonality to the chance of at least one tornado cluster (Fig. 3). The empirical seven-day probability of at least one cluster is between 20 and 30% for much of the year except between the middle of March and early July (Fig. 3A). The probabilities approach 80% between mid and late May. The number of tornadoes per cluster is less variable ranging between about 10 and 35 tornadoes per week with no strong seasonality although clusters during July and August tend to have somewhat fewer tornadoes (Fig. 3B). The casualty rate, defined as the number of casualties per 100,000 people within the cluster area, has a distinct seasonality with rates being highest between March to April and August to September (Fig. 3C).

Across the 768 clusters the mean of the maximum values of CAPE is 2,225 J kg^{-1} and the mean of the minimum values of CIN is -114 J kg^{-1} (Table 3). The maximum deep-layer bulk shear values range from 5.6 to 47.9 m s^{-1}. Cluster areas range from 361 to 1,064,337 km^2 with an average of 167,990 km^2.

b. A model for the number of tornadoes

First, we fit a negative binomial regression to the cluster-level tornado counts using the explanatory variables given in Table 3. This is our tornado-count model. We divide the cluster area by 10 million so it has units of 100 km^2. We divide CAPE by 1000 so it has units of 1000 J kg^{-1} and we divide CIN by 100 so it has units of 100 J kg^{-1}. This simplifies interpretation of the model coefficients, but does not affect the goodness of fit.

All terms have signs on the coefficient that are physically reasonable (Table 4). The number of tornadoes in a cluster increases with cluster area, CAPE, and bulk shear (deep and shallow layers) and increases for decreasing CIN (i.e., less inhibition) as expected. The significance of the variable in statistically explaining tornado counts is assessed by the corresponding z-value given as the ratio of the coefficient estimate to its standard error (S.E.). We reject the null hypothesis that a particular variable has no explanatory power if its corresponding p-value is less than .01. Here we fail to reject the null hypothesis for the variables latitude, longitude, and year, which indicates that these non-physical variables have a relatively small impact on tornado counts relative to the physical variables given the data and the model. In particular, there is no significant trend over time in the number of tornadoes in these clusters. The only physical variable that is not statistically significant is CIN. We remove all statistically insignificant variables before fitting a final model.

All variables in the final model are significant although the magnitudes of the coefficients have changed a bit relative to their values in the initial model. The in-sample correlation between the observed counts and predicted rates is .59 [(0.54, 0.64), 95% uncertainty interval (UI)] (Fig. 4). We find that the model is not improved by using the average values of these same environmental variables. The model statistically explains almost 60% of the variation in cluster-level tornado counts but tends to over predict the number of tornadoes for smaller clusters and slightly under predict the number of tornadoes for larger clusters. The mean absolute error between the observed counts and expected rates is 8.6 tornadoes or 5.2% of the range in observed counts and 9.3% of the range in predicted rates. The out-of-sample errors are quite similar due to the large sample size (768 clusters). A hold-one-out cross validation exercise (Elsner and Schmertmann 1994) results in an out-of-sample correlation of .58 and a mean absolute error of 8.6 tornadoes. The lag-1 temporal autocorrelation in cluster-level tornado counts is .13.

The value of β_0 (Table 4) is the regression estimate when all variables in the model are evaluated at zero. The effect size for a given explanatory variable is given by the magnitude of its corresponding coefficient. The coefficient is expressed as the difference in the logarithm of the expected tornado counts for a unit increase in the explanatory variable holding the other variables constant. For example, the scaled units of CAPE are 1000 J kg^{-1}. An increase in CAPE of 1000 J kg^{-1} results in a (exp(.0459) - 1) $\times$ 100% = 4.7% increase in the expected number of tornadoes, conditional on at least ten tornadoes. Continuing, units of deep-layer bulk shear are 10 m s^{-1} so an increase in shear of 10 m s^{-1} results in a 13% increase in the expected number of tornadoes. A similar increase in shallow-layer bulk shear results in a 11.1% increase in the number of tornadoes.

Changes to the expected number of tornadoes given changes in the environmental variables have a large impact on the probability distribution of counts conditional on the cluster area. The negative binomial distribution for the number of tornadoes T with an expected number of tornadoes $\bar{T}$ (obtained from the regression model) has a probability density

$$\Pr(T = k) = \frac{\Gamma(r+k)}{k!\,\Gamma(r)} \left(\frac{r}{r+\bar{T}}\right)^r \left(\frac{\bar{T}}{r+\bar{T}}\right)^k \quad \text{for } k = 10, 11, 12, \ldots, \tag{2}$$

where $r = 1/n$ and $\Gamma(z) = \int_0^\infty x^{z-1} e^{-x}\,dx$ is the gamma function.

For example, on April 12, 2020 the 12 UTC guidance from the SPC convective outlook defined an area with a 10% chance of at least one tornado occurring within 40 km of any location (10% tornado risk). The area of the polygon was approximately 400,000 km^2 (much larger than the average cluster area) centered on Mississippi (Fig. 5). With an area of that size, the model estimates the probability of at least 30 tornadoes for a range of deep-layer shear values and conditional on the amount of CAPE while holding shallow-layer shear at the average value of all clusters (Fig. 6). Given an average amount of shallow-layer shear, a deep-layer shear of 10 m s^{-1} and low CAPE (5th percentile value), the model predicts a 17% [9, 26%, UI] chance of at least 30 tornadoes (given a cluster with at least ten tornadoes). In contrast, given a deep-layer shear of 40 m s^{-1} and high CAPE (95th percentile value), the model predicts a 65% [(56, 71%), UI] chance of at least 30 tornadoes. There were more than 100 tornadoes on that day.

The model quantifies the empirical relationship between CAPE and, independently, shear in terms of a probability distribution on the number of tornadoes. It predicts the expected count given values for the explanatory variables. The negative binomial distribution uses the model's predicted count and the size parameter to generate a distribution of probabilities. For example, the model gives predicted probabilities across a range of CAPE and deep-layer shear values (holding shallow-layer shear at its mean value) that provides a picture of the relationship (Fig. 7). The predicted probabilities of at least 30 tornadoes given an outbreak covering an area of 400,000 km^2 increase from low values of both CAPE and shear to high values of both CAPE and shear.

c. A model for the number of casualties

Next we fit a negative binomial regression to the cluster-level casualty counts (direct injuries and deaths) using the same explanatory variables (Table 3) with the exceptions that population (scaled by 100,000 residents) replaces cluster area and C (casualty count) replaces T (tornado count) as the dependent variable. This is our casualty-count model. We find that CIN is the only variable not significant in the initial model (Table 5). We remove it before fitting a final model.

The in-sample correlation between the observed casualty counts and predicted rates is .43 [(.37, .48), 95% UI] (Fig. 8). The mean absolute error between the observed counts and expected rates is 39 casualties or 1.3% of the range in observed counts and 3.4% of the range in predicted rates. The out-of-sample correlation is .36 and the mean absolute error is 40 casualties. The skill is lower than the skill of the tornado-count model as there is additional uncertainty associated with the number of casualties given a tornado.

As expected from the tornado-count model, the number of casualties resulting from a cluster of tornadoes increases with CAPE and with the two bulk shear variables (Table 5) which is consistent with Anderson-Frey and Brooks (2019). Holding all other variables constant, an increase in CAPE of 1000 J kg^{-1} results in a 28% increase in the expected number of casualties. An increase in deep-layer bulk shear of 10 m s^{-1} results in a 98% increase in the expected number of casualties per cluster and a similar increase in shallow-layer bulk shear results in a 76% increase in the expected number of casualties per cluster, conditional on at least ten tornadoes. Additionally, the model indicates that casualties decrease at a rate of 3.6% per year. This is very likely the result of improvements made by the National Weather Service in warning coordination and dissemination leading to better awareness especially for these large outbreak events.

Also, as expected, the number of people in harm's way is a significant explanatory variable for the cluster-level casualty count. The relationship between population and number of casualties is quantified at the tornado-level in Elsner et al. (2018) and Fricker et al. (2017) so we expect the relationship to hold at the cluster level. Here, we are able to compare the influence of shear and CAPE on the probability of casualties as modulated by population (Fig. 9). Model results are shown for three levels of population. The probability of a large number of casualties increases with increasing shear and increasing CAPE, while keeping the other variables at their mean values and year at 2018.

Importantly, we also find that where the cluster occurs has a significant influence on the number of casualties consistent with other studies (Ashley and Strader 2016; Fricker and Elsner 2019). For every one degree north latitude the casualty rate decreases by 5.5% and for every one degree east longitude the casualty rate increases by 2.9%. Thus, cluster-level casualties are highest over the Southeast. This effect is independent of the number of tornadoes since location was not a significant factor in the tornado-count model. The result is also independent of the number of people in harm's way since population is included as an exploratory variable in the model.

To visualize the difference of the combined effects of latitude and longitude on the difference in the probability of many casualties, we plot modeled casualty probabilities (at least 25) as a function of CAPE and deep-layer shear for two *hypothetical* outbreaks that are the same in every way except one outbreak is centered on Sioux City, Iowa (42.5° N, 96.4° W), and the other is centered on Birmingham, Alabama (33.5° N, 86.8° W) (Fig. 10). The modeled probabilities are lowest (around 5%) for low CAPE and shear values and highest (above 30%) for high CAPE and shear values.

The difference in modeled probabilities across these two locations peaks at about +12 percentage points for high CAPE and high shear regimes when the outbreak is centered on Birmingham.

4. Summary and conclusions

Estimating characteristics of severe weather outbreaks (e.g., tornado and casualty counts) is challenging but important. Forecasters use a combination of numerical weather prediction and empirical guidance to outline areas of severe convective weather. Here we demonstrate a statistical regression model that can take advantage of the large sample of independent tornado 'outbreaks' as a way to statistically explain the number of tornadoes and the number of casualties in a cluster of at least ten tornadoes. We fit negative binomial regressions to tornado characteristics aggregated to the level of tornado clusters where a cluster is a space-time group of at least ten tornadoes occurring between 12 UTC and 12 UTC over the period 1994–2018. The number of tornadoes in each cluster is the response variable in the tornado-count model, and the number of casualties (deaths plus injuries) is the response variable in the casualty-count model. Environmental explanatory variables for the models are extracted from reanalysis data representing conditions before the occurrence of the first tornado in the cluster consistent with Schroder and Elsner (2019). Additional explanatory variables include cluster area, population, location, and year.

The estimated tornado rates, conditional on there being at least ten tornadoes, explain 59% of the observed tornado counts in-sample, and the estimated casualty rates explain 43% of the observed casualty counts in-sample. Because of the large sample size, the out-of-sample skill is lower but still useful. The models show that a 1000 J kg^{-1} increase in CAPE results in a 4.7% increase in the expected number of tornadoes conditional on at least ten tornadoes and a 28% increase in the expected number of casualties, holding the other variables constant. The models further show that a 10 m s^{-1} increase in deep-layer bulk shear results in a 13% increase in the expected number of tornadoes and a 98% increase in the expected number of casualties, holding the other variables constant while a recent study showed the number of tornadoes and casualties increase with both CAPE and shear (Anderson-Frey and Brooks 2019). This study quantifies these increases. The casualty-count model also shows a significant decline in the number of casualties at a rate of 3.6% per year. Casualty rates depend on where the outbreak occurs with more deaths and injuries, on average, over the Southeast, controlling for the other variables; a result that is consistent with the recent work of Fricker and Elsner (2019) and Biddle et al. (2020).

Some of the unexplained variability in cluster-level tornado counts (and casualty counts) arises from the uncertainty associated with the preferred storm mode and the evolution of meso-scale convective systems, neither of which are captured by a single maximum value in the variable space of CAPE and shear. The counts are also limited by the quality of the NARR data. The NARR tends to unrealistically favor tornado environments during specific convective setups (Gensini and Ashley 2011; Gensini et al. 2014; Allen et al. 2015a). Also, outbreaks associated with tropical cyclones likely add a bit of noise to both models since the number of tornadoes is sensitive to the extent and location of convective bursts within overall evolution of the land-falling storm.

The casualty-count model would be improved by including a skillful estimate of the number of tornadoes. Indeed in a perfect-prognostic setting, where we know the number of tornadoes in the outbreak, the out-of-sample correlation between the observed number of casualties and the modeled estimated rate of casualties increases to .79. Further, although our approach to extracting signal from noise in the tornado dataset is sound, exclusive focus on clusters with at least ten tornadoes is a type of selection bias meaning that the sample of data used to fit the model does not represent the population of all outbreaks, which limits what we can say in general about the effect of convective environments on the probability distribution of casualty counts.

The casualty-count model can be employed in a research setting to help better understand the socioeconomic, demographic, and communication factors that make some communities particularly vulnerable to deaths and injuries (Dixon and Moore 2012; Senkbeil et al. 2013; Klockow et al. 2014; Fricker and Elsner 2019). Work along this line has been done at the individual tornado level by identifying unusually devastating events (Fricker and Elsner 2019), but scaling this type of analysis to the cluster-level to identify unusually devastating outbreaks might provide additional insights.

Finally, it is possible that the models could be improved by including nonlinear effects. One type of non-linearity is interaction where the effect of CAPE on casualties is modulated by shear, for example. However, interaction effects usually must be specified without reference to the data, so additional research on this is needed. The models also might be improved by adjusting the threshold definition of a cluster. Increasing the threshold on the tornado-count model from 10 to 14 decreases the sample size to 505 clusters and reduces the effect sizes on CAPE and shear by around 25%. Decreasing the threshold from 10 to 6 increases the sample size and, thus, reduces the standard error assuming the effect size stays the same. A casualty-count model might also be improved by relaxing the assumption that the numbers of people injured or killed are independent. Casualty counts are typically not independent at the household level where multiple people live under the same roof. In this case a better probability model for the data might be a zero-inflated count process rather than a negative binomial process as used here.

Acknowledgments. The negative binomial regression models in this paper were implemented with the `glm.nb` function from the `MASS` R package (Venables and Ripley 2002). Graphics were made with the `ggplot2` framework (Wickham 2017). The code and data to fit all the models is available on GitHub (https://github.com/jelsner/cape-shear).

References

Allen, J. T., M. K. Tippett, and A. H. Sobel, 2015a: An empirical model relating U.S. monthly hail occurrence to large-scale meteorological environment. *Journal of Advances in Modeling Earth Systems*, **7 (1)**, 226–243, doi:10.1002/2014MS000397, URL https://agupubs.onlinelibrary.wiley.com/doi/abs/10.1002/2014MS000397.

Allen, J. T., M. K. Tippett, and A. H. Sobel, 2015b: Influence of the El Niño/Southern Oscillation on tornado and hail frequency in the United States. *Nature Geosciences*, **8**, 278–283.

Anderson-Frey, A. K., and H. Brooks, 2019: Tornado fatalities: An environmental perspective. *Weather and Forecasting*, **34 (6)**, 1999–2015, doi:10.1175/waf-d-19-0119.1, URL https://doi.org/10.1175/waf-d-19-0119.1.

Anderson-Frey, A. K., Y. P. Richardson, A. R. Dean, R. L. Thompson, and B. T. Smith, 2018: Near-storm environments of outbreak and isolated tornadoes. *Weather and Forecasting*, **33 (5)**, 1397–1412, doi:10.1175/WAF-D-18-0057.1, URL https://doi.org/10.1175/WAF-D-18-0057.1, https://doi.org/10.1175/WAF-D-18-0057.1.

Ashley, W. S., and S. M. Strader, 2016: Recipe for disaster: How the dynamic ingredients of risk and exposure are changing the tornado disaster landscape. *Bulletin of the American Meteorological Society*, **97**, 767–786.

Biddle, M. D., R. P. Brown, C. A. Doswell, and D. R. Legates, 2020: Regional differences in the human toll from tornadoes: A new look at an old idea. *Weather, Climate, and Society*, **12 (4)**, 815–825, doi:10.1175/wcas-d-19-0051.1, URL https://doi.org/10.1175/wcas-d-19-0051.1.

Brooks, H. E., G. W. Carbin, and P. T. Marsh, 2014: Increased variability of tornado occurrence in the United States. *Science*, **346 (6207)**, 349–352, doi:10.1126/science.1257460, URL https://science.sciencemag.org/content/346/6207/349, https://science.sciencemag.org/content/346/6207/349.full.pdf.

Brooks, H. E., C. A. Doswell , and J. Cooper, 1994: On the environments of tornadic and nontornadic mesocyclones. *Weather and Forecasting*, **9**, 606–618, doi:10.1175/1520-0434.

Cohen, A. E., J. B. Cohen, R. L. Thompson, and B. T. Smith, 2018: Simulating tornado probability and tornado wind speed based on statistical models. *Weather and Forecasting*, **33 (4)**, 1099–1108, doi:10.1175/waf-d-17-0170.1, URL https://doi.org/10.1175/waf-d-17-0170.1.

Concannon, P., H. E. Brooks, and C. A. Doswell , 2000: Climatological risk of strong and violent tornadoes in the United States. *Second Conference on Environmental Applications*.

Dean, A. R., 2010: P2.19 An analysis of clustered tornado events. *25th Conference on Severe Local Storms*.

Dixon, P. G., A. E. Mercer, K. Grala, and W. H. Cooke, 2014: Objective identification of tornado seasons and ideal spatial smoothing radii. *Earth Interactions*, **18**, 1–15.

Dixon, R. W., and T. W. Moore, 2012: Tornado vulnerability in Texas. *Weather, Climate, and Society*, **4**, 59–68.

Doswell, C. A., R. Edwards, R. L. Thompson, J. A. Hart, and K. C. Crosbie, 2006: A simple and flexible method for ranking severe weather events. *Weather and Forecasting*, **21 (6)**, 939–951, doi:10.1175/waf959.1, URL https://doi.org/10.1175/waf959.1.

Elsner, J. B., S. C. Elsner, and T. H. Jagger, 2015: The increasing efficiency of tornado days in the United States. *Climate Dynamics*, **45 (3-4)**, 651–659.

Elsner, J. B., T. Fricker, and W. D. Berry, 2018: A model for U.S. tornado casualties involving interaction between damage path estimates of population density and energy dissipation. *Journal of Applied Meteorology and Climatology*, **57**, 2035–2046.

Elsner, J. B., and C. P. Schmertmann, 1994: Assessing forecast skill through cross validation. *Weather and Forecasting*, **9 (4)**, 619–624.

Elsner, J. B., and Z. Schroder, 2019: Tornado damage ratings estimated with cumulative logistic regression. *Journal of Applied Meteorology and Climatology*, **58 (12)**, 2733–2741, doi:10.1175/jamc-d-19-0178.1, URL https://doi.org/10.1175/jamc-d-19-0178.1.

Fricker, T., and J. B. Elsner, 2019: Unusually devastating tornadoes in the United States: 1995–2016. *Annals of the American Association of Geographers*, **110 (3)**, 724–738, doi:10.1080/24694452.2019.1638753, URL https://doi.org/10.1080/24694452.2019.1638753.

Fricker, T., J. B. Elsner, and T. H. Jagger, 2017: Population and energy elasticity of tornado casualties. *Geophysical Research Letters*, **44**, 3941–3949, doi:10.1002/2017GL073093.

Fujita, T. T., 1981: Tornadoes and downbursts in the context of generalized planetary scales. *J. Atmos. Sci.*, **38**, 1511–1534.

Galway, J. G., 1977: Some climatological aspects of tornado outbreaks. *Monthly Weather Review*, **105**, 477–484.

Gensini, V., and W. Ashley, 2011: Climatology of potentially severe convective environments from the North American Regional Reanalysis. *Electronic Journal of Severe Storms Meteorology*, **6**, 1–40, doi:10.1038/s41612-018-0048-2.

Gensini, V. A., T. L. Mote, and H. E. Brooks, 2014: Severe-thunderstorm reanalysis environments and collocated radiosonde observations. *Journal of Applied Meteorology and Climatology*,

53 (3), 742–751, doi:10.1175/jamc-d-13-0263.1, URL https://doi.org/10.1175/jamc-d-13-0263.1.

Heiss, W. H., D. L. McGrew, and D. Sirmans, 1990: NEXRAD: next generation weather radar (WSR-88D). *Microwave Journal*, **33 (1)**, 79.

Hilbe, J., 2011: *Negative Binomial Regression*. Cambridge University Press.

Hill, A. J., G. R. Herman, and R. S. Schumacher, 2020: Forecasting severe weather with random forests. *Monthly Weather Review*, doi:10.1175/mwr-d-19-0344.1, URL https://doi.org/10.1175/mwr-d-19-0344.1.

Hitchens, N. M., and H. E. Brooks, 2014: Evaluation of the Storm Prediction Center's convective outlooks from day 3 through day 1. *Weather and Forecasting*, **29 (5)**, 1134–1142, doi:10.1175/waf-d-13-00132.1, URL https://doi.org/10.1175/waf-d-13-00132.1.

Jackson, J. D., and M. E. Brown, 2009: Sounding-derived low-level thermodynamic characteristics associated with tornadic and non-tornadic supercell environments in the Southeast United States. *National Weather Digest*, **33**, 16–26.

Klockow, K. E., R. A. Peppler, and R. A. McPherson, 2014: Tornado folk science in Alabama and Mississippi in the 27 April 2011 tornado outbreak. *GeoJournal*, **79 (6)**, 791–804, doi:10.1007/s10708-013-9518-6, URL https://doi.org/10.1007/s10708-013-9518-6.

Mesinger, F., and Coauthors, 2006: North American Regional Reanalysis. *Bulletin of the American Meteorological Society*, **87 (3)**, 343–360, doi:10.1175/BAMS-87-3-343, URL https://doi.org/10.1175/BAMS-87-3-343, https://doi.org/10.1175/BAMS-87-3-343.

Moore, T., 2017: On the temporal and spatial characteristics of tornado days in the United States. *Atmospheric Research*, **184**, doi:10.1016/j.atmosres.2016.10.007.

Moore, T. W., R. W. Dixon, and N. J. Sokol, 2016: Tropical cyclone Ivan's tornado cluster in the Mid-Atlantic region of the United States on 17–18 September 2004. *Physical Geography*, **37 (3-4)**, 210–227, doi:10.1080/02723646.2016.1189299, URL https://doi.org/10.1080/02723646.2016.1189299.

Rasmussen, E. N., and D. O. Blanchard, 1998: A baseline climatology of sounding-derived supercell and tornado forecast parameters. *Weather and Forecasting*, **13 (4)**, 1148–1164, doi:10.1175/1520-0434(1998)013<1148:ABCOSD>2.0.CO;2, URL https://doi.org/10.1175/1520-0434(1998)013<1148:ABCOSD>2.0.CO;2.

Schroder, Z., and J. B. Elsner, 2019: Quantifying relationships between environmental factors and power dissipation on the most prolific days in the largest tornado "outbreaks". *International Journal of Climatology*, doi:10.1002/joc.6388, URL https://doi.org/10.1002/joc.6388.

Senkbeil, J. C., D. A. Scott, P. Guinazu-Walker, and M. S. Rockman, 2013: Ethnic and racial differences in tornado hazard perception, preparedness, and shelter lead time in Tuscaloosa. *The Professional Geographer*, **66 (4)**, 610–620, doi:10.1080/00330124.2013.826562, URL https://doi.org/10.1080/00330124.2013.826562.

Shafer, C. M., and C. A. Doswell, 2011: Using kernel density estimation to identify, rank, and classify severe weather outbreak events. *Electronic Journal of Severe Storms Meteorology*, **6**, 1–28.

Steiner, E., 2019: Spatial history project. Center for Spatial and Textual Analysis, Stanford University, URL http://web.stanford.edu/group/spatialhistory/cgi-bin/site/index.php.

Thompson, R. L., R. Edwards, J. A. Hart, K. L. Elmore, and P. Markowski, 2003: Close proximity soundings within supercell environments obtained from the Rapid Update Cycle. *Weather* *and Forecasting*, **18 (6)**, 1243–1261, doi:10.1175/1520-0434(2003)018<1243:cpswse>2.0.co;2, URL https://doi.org/10.1175/1520-0434(2003)018<1243:cpswse>2.0.co;2.

Thompson, R. L., and Coauthors, 2017: Tornado damage rating probabilities derived from WSR-88D data. *Weather and Forecasting*, **32 (4)**, 1509–1528, doi:10.1175/waf-d-17-0004.1, URL https://doi.org/10.1175/waf-d-17-0004.1.

Tippett, M. K., C. Lepore, and J. E. Cohen, 2016: More tornadoes in the most extreme U.S. tornado outbreaks. *Science*, **354 (6318)**, 1419–1423, doi:10.1126/science.aah7393, URL https://doi.org/10.1126/science.aah7393.

Tippett, M. K., A. H. Sobel, and S. J. Camargo, 2012: Association of U.S. tornado occurrence with monthly environmental parameters. *Geophysical Research Letters*, **39**, L02 801.

Venables, W. N., and B. D. Ripley, 2002: *Modern Applied Statistics with S*. 4th ed., Springer, New York, URL http://www.stats.ox.ac.uk/pub/MASS4, iSBN 0-387-95457-0.

Wickham, H., 2017: *tidyverse: Easily Install and Load 'Tidyverse' Packages*. URL https://CRAN.R-project.org/package=tidyverse, r package version 1.1.1.

LIST OF TABLES

Table 1. Cluster statistics by time of day. Each cluster is categorized by the closest three-hour time (defined by the NARR data) prior to the first tornado.

Time of Day (UTC)	Number of Clusters	Number of Tornadoes	Average Tornadoes Per Cluster	Average Duration (hours)
00	33	523	15.8	6.1
03	5	67	13.4	6.4
06	2	23	11.5	3.2
12	145	3598	12.1	14.0
15	124	3222	26.0	11.5
18	249	5220	21.0	8.4
21	210	4416	21.0	7.0

TABLE 2. Correlation matrix of environmental variables considered in this study. Dew-point temperature (DEW), specific humidity (SH), and storm relative helicity (HLCY). Only CAPE, CIN, DLBS, and SLBS are used as explanatory variables in the models.

	CAPE	CIN	DLBS	SLBS	HLCY	DEW	SH
CAPE	1.00						
CIN	-0.07	1.00					
DLBS	-0.03	-0.29	1.00				
SLBS	-0.37	-0.24	0.49	1.00			
HLCY	-0.22	-0.30	**0.58**	**0.76**	1.00		
DEW	**0.56**	0.00	-0.08	0.02	-0.08	1.00	
SH	**0.64**	0.00	-0.12	-0.08	-0.13	**0.98**	1.00

TABLE 3. Variables considered in the regression models. Values include the range and average across the 768 tornado clusters.

Variable	Abbreviation	Range	Average
Explanatory Variables			
Convective Available Potential Energy [J kg^{-1}]	CAPE	[0, 6530]	2225
Convective Inhibition [J kg^{-1}]	CIN	[−668, 0]	−114
Deep-Layer Bulk Shear [m s^{-1}]	DLBS	[5.6, 48]	27.5
Shallow-Layer Bulk Shear [m s^{-1}]	SLBS	[1.1, 33.8]	15.0
Latitude [° N]	ϕ	[27.12, 48.97]	37.20
Longitude [° E]	λ	[−109.9 −72.88]	−92.16
Cluster Area [km^2]	A	[361, 1,064,337]	167,990
Population [No. of People]	P	[0, 38,226,946]	3,387,259
Year	Y	[1994, 2018]	2006
Response Variables			
Number of Tornadoes	T	[10, 173]	22.2
Number of Casualties (injuries plus deaths)	C	[0, 3,069]	29.9

TABLE 4. Coefficients in the tornado-count models. The size parameter (n) is 6.27 ± .393 (standard error) for the initial model 6.25 ± .392 (standard error) for the final model.

Coefficient	Estimate	S.E.	z value	Pr(>|z|)
		Initial Model		
β_0	4.5489	4.7662	0.9540	0.3399
β_A	0.0146	0.0011	12.80	< 0.0001
β_ϕ	−0.0051	0.0043	−1.17	0.2427
β_λ	−0.0028	0.0031	−0.917	0.3594
β_Y	−0.0012	0.0024	−0.515	0.6068
β_{CAPE}	0.0452	0.0153	2.96	0.0031
β_{CIN}	−0.0110	0.0189	−0.581	0.5612
β_{DLBS}	0.1256	0.0292	4.30	< 0.0001
β_{SLBS}	0.1059	0.0355	2.98	0.0029
		Final Model		
β_0	2.1779	0.0817	26.65	< 0.0001
β_A	0.0149	0.0011	13.85	< 0.0001
β_{CAPE}	0.0459	0.0146	3.13	0.0017
β_{DLBS}	0.1254	0.0288	4.35	< 0.0001
β_{SLBS}	0.1054	0.0314	3.35	0.0008

TABLE 5. Coefficients in the casualty-county models. The size parameter (n) is .261 ± .014 (standard error) for the initial and final models.

Coefficient	Estimate	S.E.	z value	Pr(>|z|)
		Initial Model		
β_0	76.6908	20.7430	3.70	0.0002
β_P	0.0122	0.0019	6.51	< 0.0001
β_ϕ	−0.0561	0.0187	−3.00	0.0027
β_λ	0.0284	0.0136	2.09	0.0363
β_Y	−0.0364	0.0103	−3.52	0.0004
β_{CAPE}	0.2436	0.0643	3.79	0.0002
β_{CIN}	0.0052	0.0802	0.07	0.9479
β_{DLBS}	0.6853	0.1262	5.43	< 0.0001
β_{SLBS}	0.5650	0.1534	3.68	0.0002
		Final Model		
β_0	76.7677	20.6902	3.71	0.0002
β_P	0.0122	0.0018	6.67	0.0000
β_ϕ	−0.0563	0.0186	−3.02	0.0025
β_λ	0.0287	0.0130	2.20	0.0277
β_Y	−0.0364	0.0103	−3.53	0.0004
β_{CAPE}	0.2440	0.0643	3.79	0.0001
β_{DLBS}	0.6833	0.1253	5.45	0.0000
β_{SLBS}	0.5631	0.1504	3.74	0.0002

LIST OF FIGURES

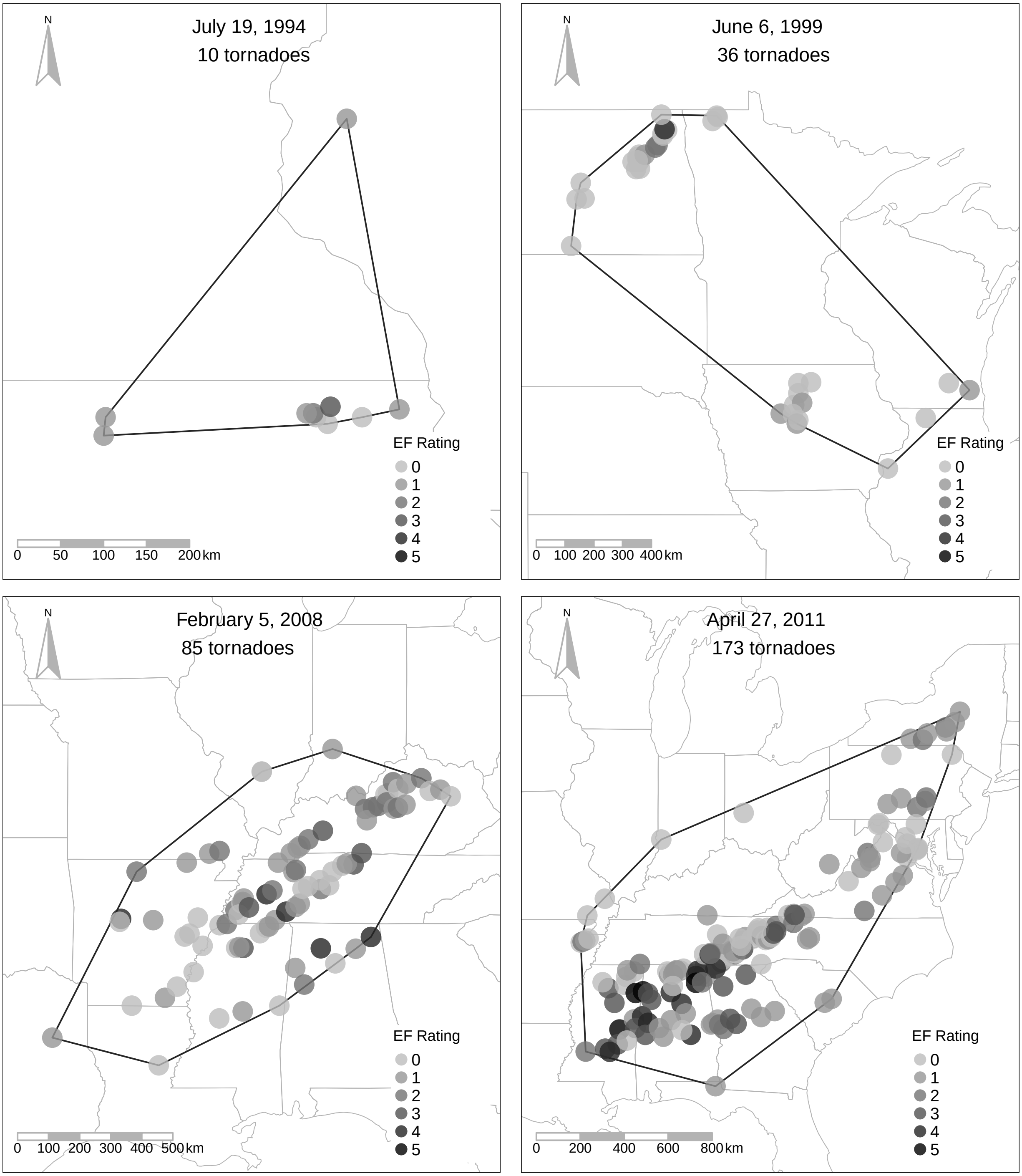

FIG. 1. Example tornado clusters. Each point is the tornadogenesis location shaded by EF rating. The black line is the spatial extent of the tornadoes occurring on that convective day and is defined by the minimum convex hull encompassing the set of locations.

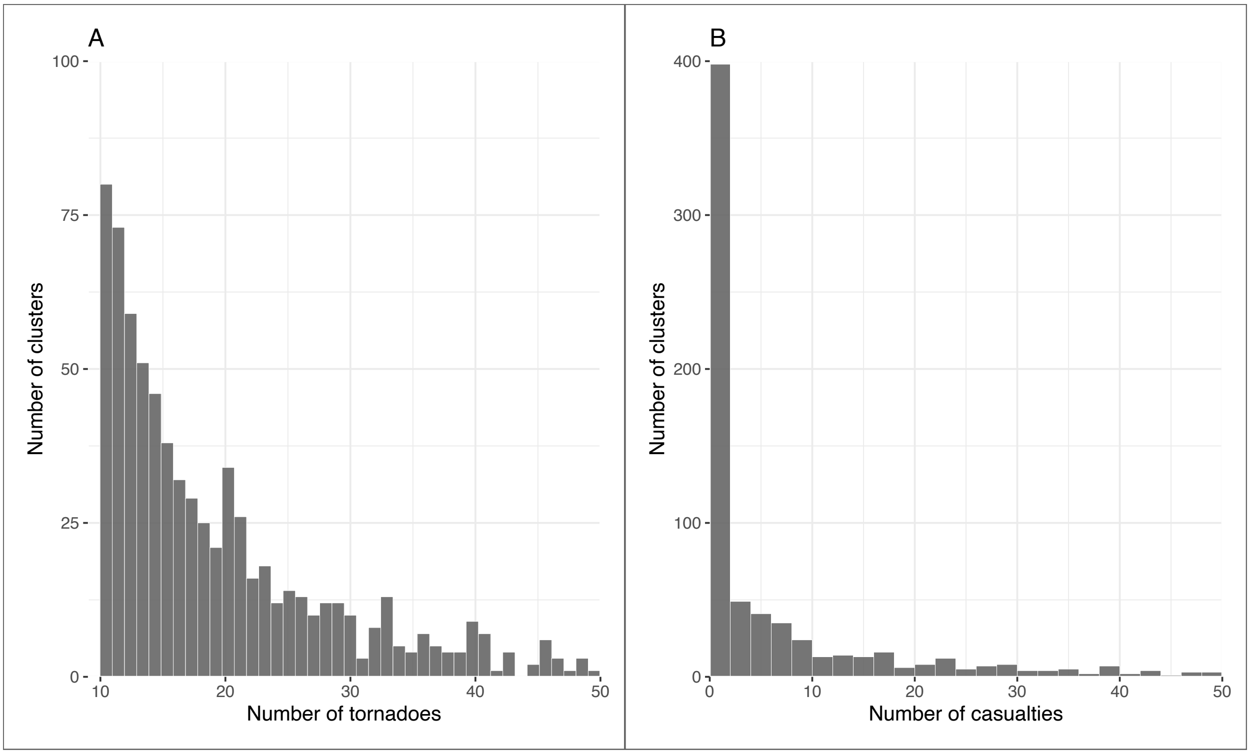

Fig. 2. Histograms of the number of clusters by number of tornadoes (A) and number of clusters by number of casualties (B). The histograms are right-truncated at 50 to show detail on the left side of the distributions. Only clusters with at least ten tornadoes are considered in this study.

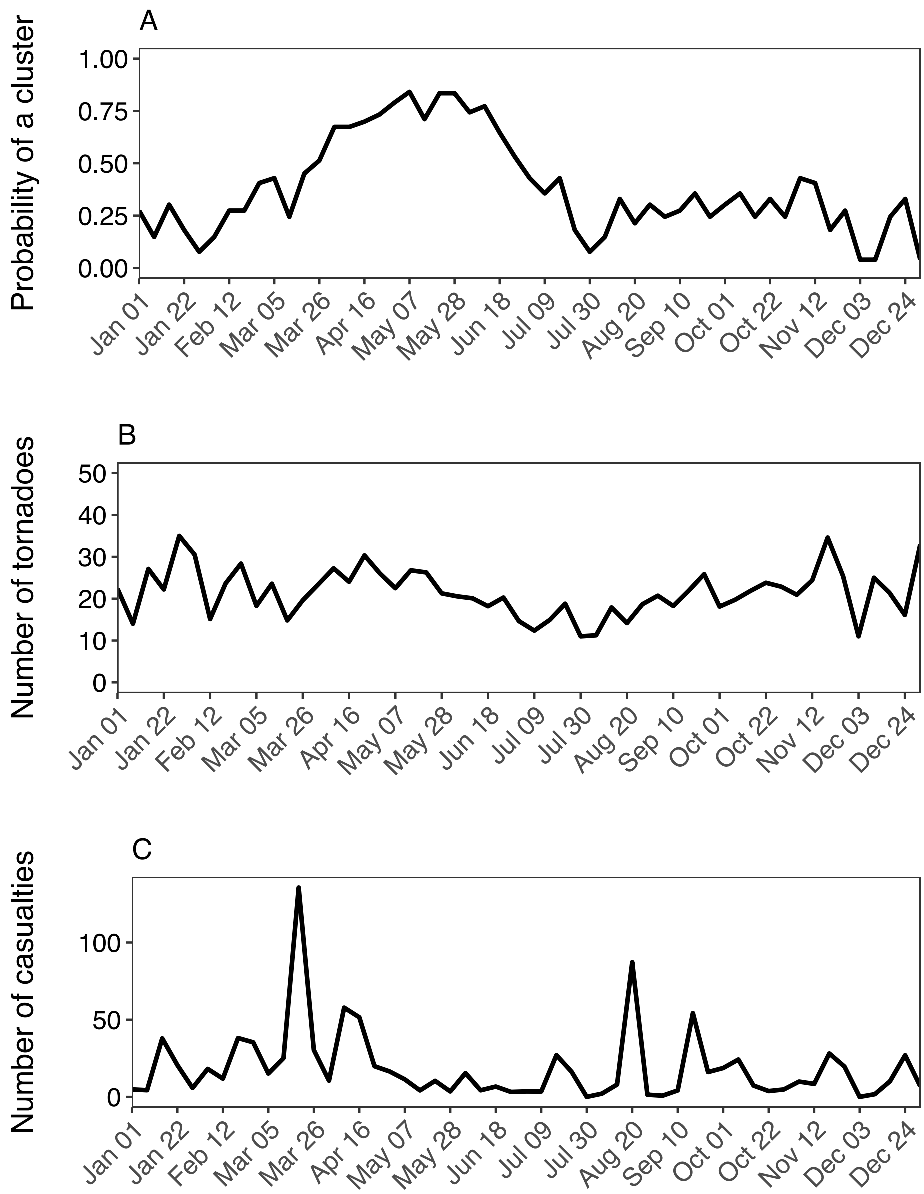

Fig. 3. Probability of a cluster (A), average number of tornadoes per cluster (B), and average number of casualties per 1 000 000 people per cluster (C) by week of the year.

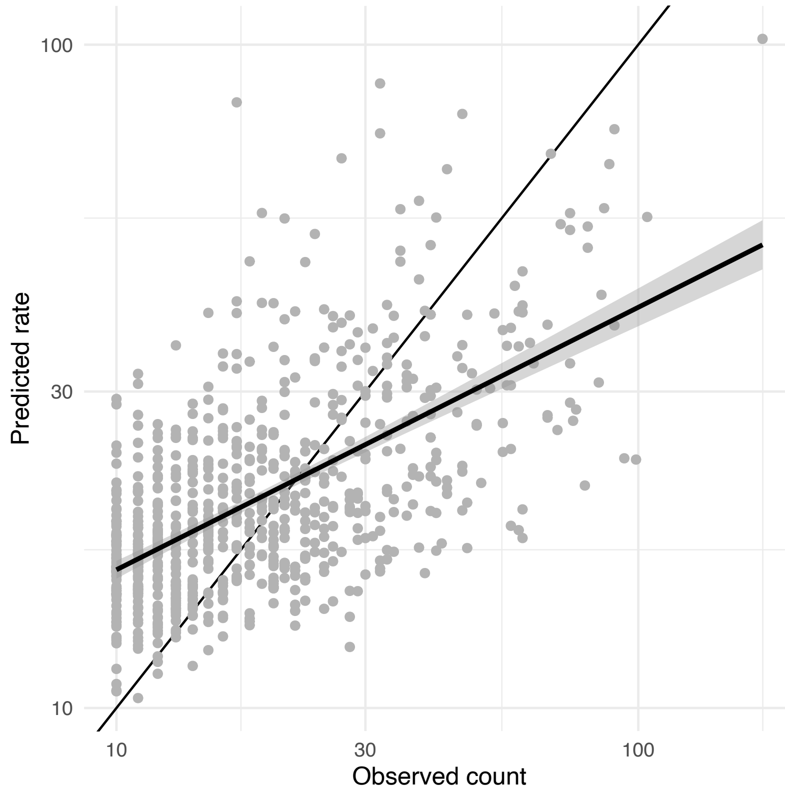

578 FIG. 4. Observed cluster-level tornado counts versus predicted rates from a negative binomial regression. The thin black line is the line of best fit. The thick line is the slope of the model indicating the relationship between the observed and predicted tornado counts and the associated standard error.

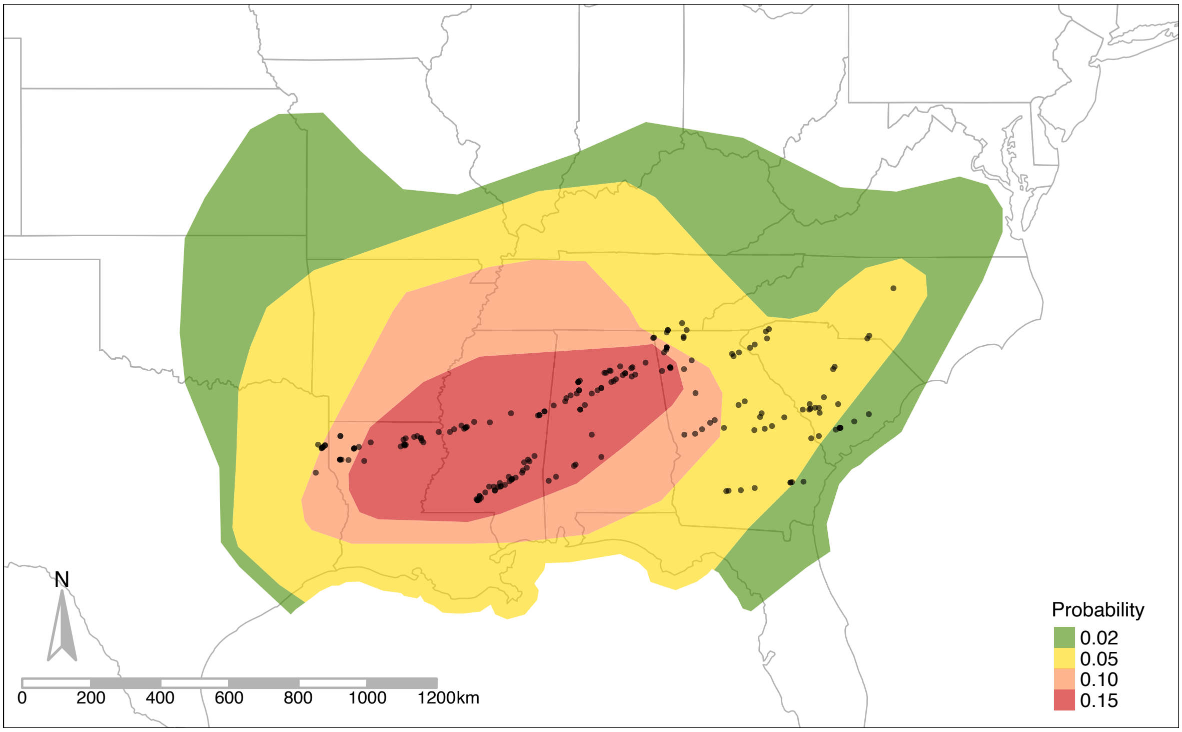

581 Fig. 5. Convective outlook issued by the Storm Prediction Center at 12 UTC on April 12, 2020 and the locations of tornado reports over the 24-hr period starting at that time. The outlook category numbers indicate the chance of observing severe weather within 40 km of any location. The convective outlook shapefiles are from `www.spc.noaa.gov/cgi-bin-spc/getacrange.pl?date0=20200412&date1=20200412` and the tornado reports are from `www.spc.noaa.gov/climo/reports/200412_rpts.html`.

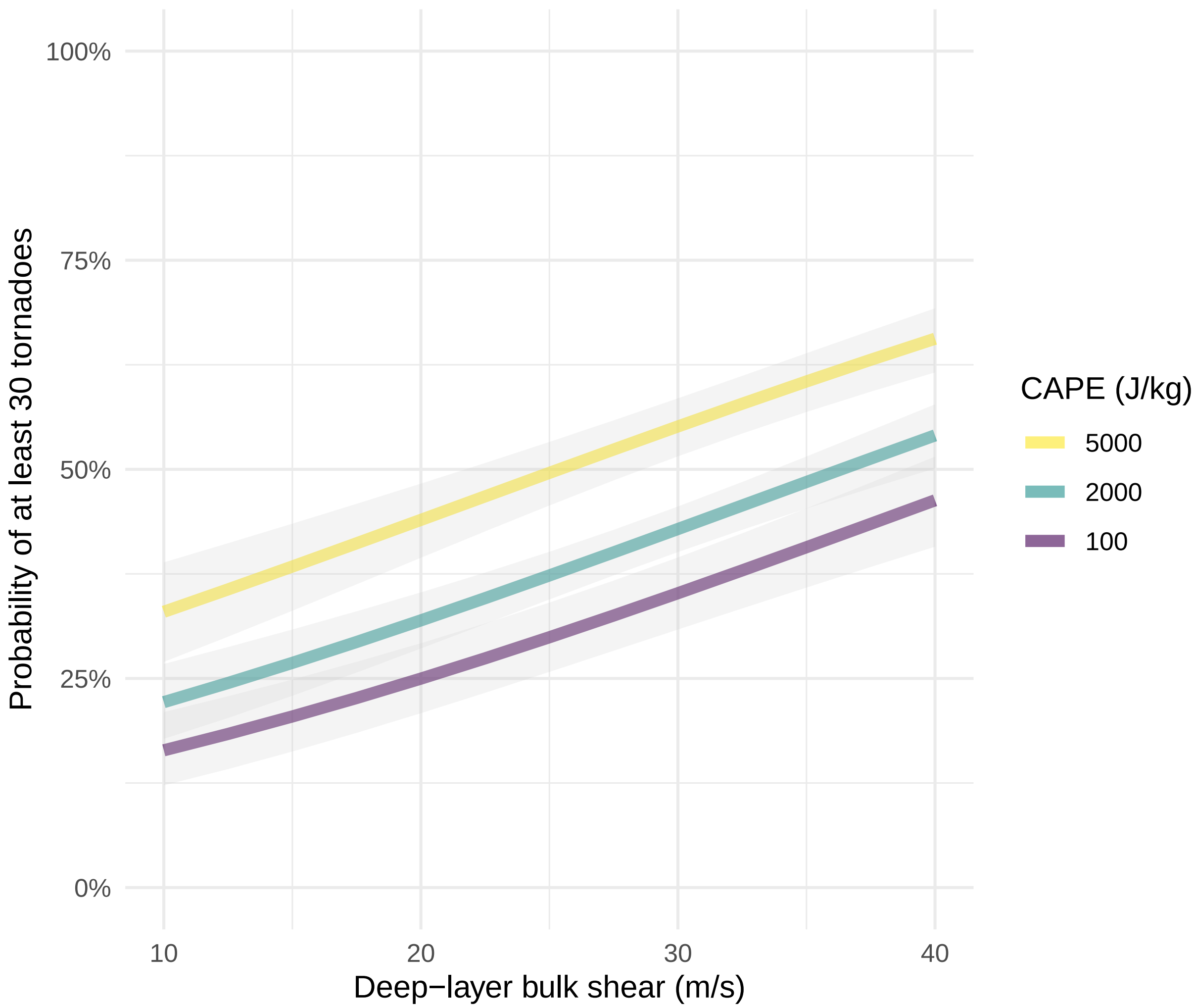

Fig. 6. Estimated probability of at least 30 tornadoes given an outbreak of at least ten tornadoes and the regression model. The predicted count from the model is a parameter in a negative binomial distribution with cluster area set at 400,000 km^2 and shallow-level bulk shear is set to its mean value.

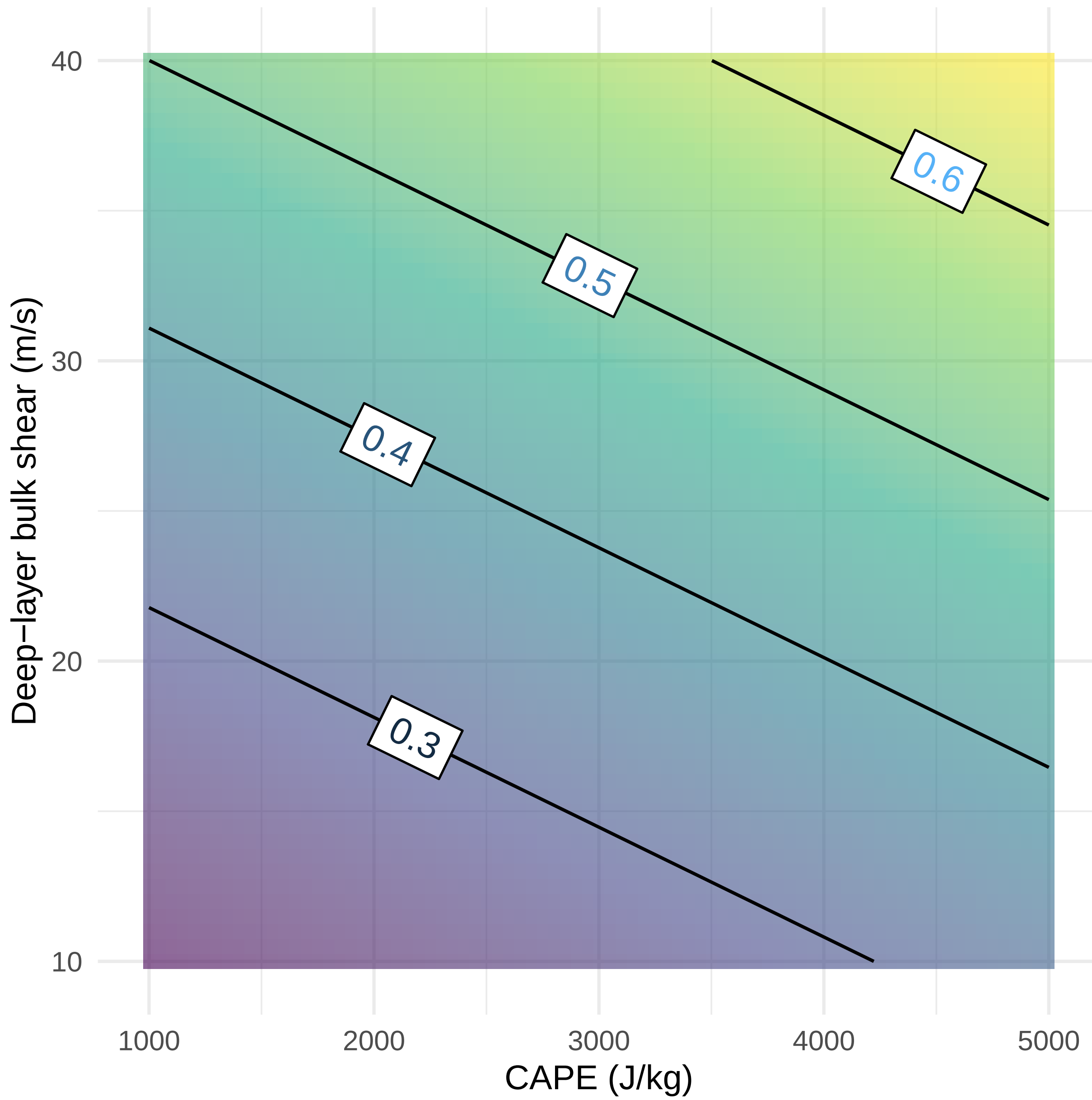

Fig. 7. Estimated probability of at least 30 tornadoes given an outbreak of at least ten tornadoes and the regression model across a range of CAPE and deep-layer bulk shear values holding the shallow-layer bulk shear at a mean value.

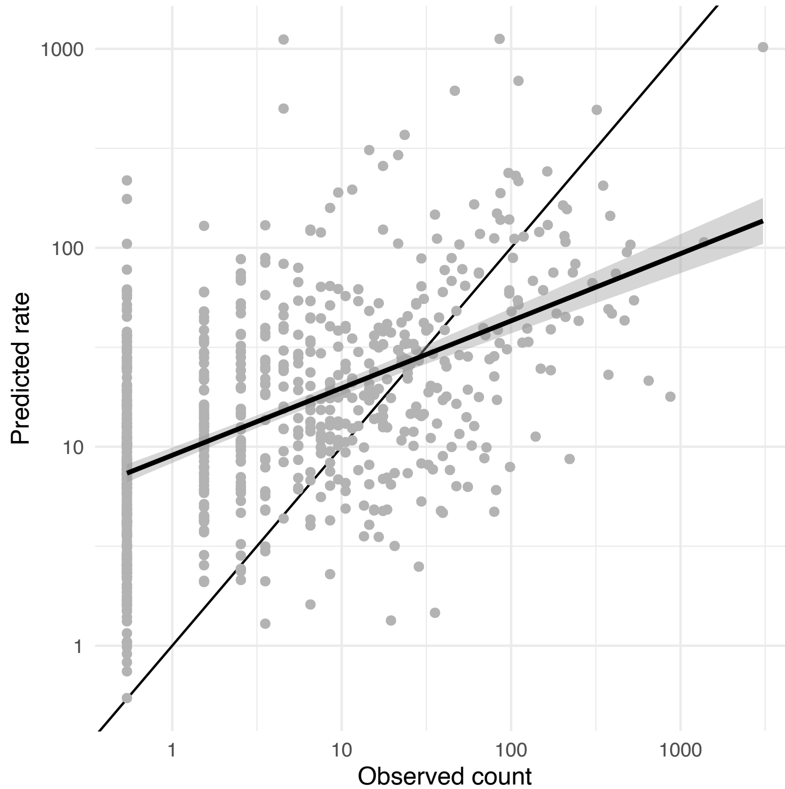

Fig. 8. Observed cluster-level casualty counts versus predicted rates from a negative binomial regression. Clusters without casualties are plotted at the far left. The thin black line is the line of best fit. The thick line is the slope of the model indicating the relationship between the observed and predicted tornado counts and the associated standard error.

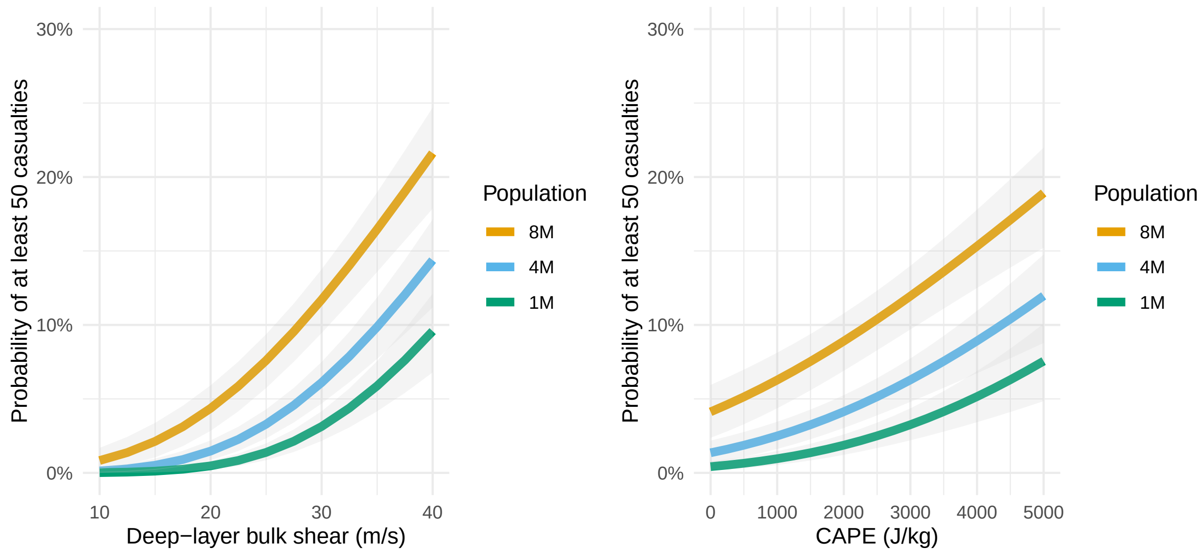

596 FIG. 9. Probability of at least 50 tornado casualties as a function of deep-layer bulk shear (left panel) and
597 CAPE (right panel) and modulated by the number of people in harm's way. The other variables are set at their
598 mean values and year is set at 2018.

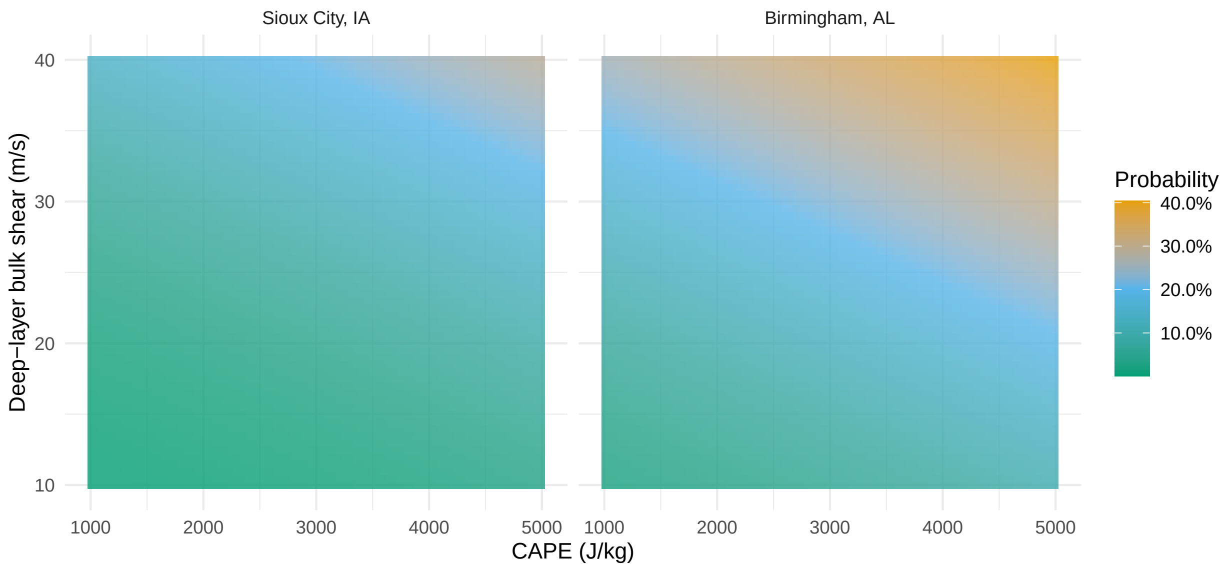

599 FIG. 10. Probability of at least 25 tornado casualties as a function of deep-layer bulk shear and CAPE and
600 modulated by location for two *hypothetical* outbreaks, one centered over Sioux City, Iowa, and the other centered
601 over Birmingham, Alabama. The shallow-layer bulk shear is set to its mean value, year is set to 2018, and
602 population is set to 4M.